Sensors and Actuators B 181 (2013) 743–748

Contents lists available at SciVerse ScienceDirect

Sensors and Actuators B: Chemical

journal homepage: www.elsevier.com/locate/snb

A pyrene-based highly selective turn-on fluorescent sensor for copper(II) ions and its application in living cell imaging

Hsuan-Fu Wang, Shu-Pao Wu*

Department of Applied Chemistry, National Chiao Tung University, Hsinchu 300, Taiwan, ROC

ARTICLE INFO

Article history:
Received 29 October 2012
Received in revised form
24 December 2012
Accepted 24 January 2013
Available online 4 February 2013

Keywords:
Sensors
Copper
Pyrene
Imaging agents

ABSTRACT

A new pyrene derivative (**1**) containing a benzothiazolenhydrazone moiety exhibited high selectivity for Cu^{2+} detection. In the presence of Cu^{2+}, chemosensor **1** provided significant fluorescence enhancement, while Ag^{+}, Ca^{2+}, Cd^{2+}, Co^{2+}, Fe^{2+}, Fe^{3+}, Hg^{2+}, K^{+}, Mg^{2+}, Mn^{2+}, Ni^{2+}, Pb^{2+}, and Zn^{2+} metal ions produced only minor changes in fluorescence intensity. The association constant (K_a) for Cu^{2+} binding to 1 had a value of $5.00 \times 10^8\ M^{-2}$. The maximum fluorescence enhancement induced by Cu^{2+} binding to the chemosensor was observed over the range pH 2–8.5. Our fluorescence microscopy experiments demonstrate that chemosensor **1** may have application as a fluorescent probe for detecting Cu^{2+} in living cells.

1. Introduction

The development of fluorescent chemosensors that are capable of detecting biologically or environmentally important metal ions such as Cd^{2+}, Cu^{2+}, Fe^{3+}, Hg^{2+}, Pb^{2+}, and Zn^{2+} has been an important research topic [1–6]. Copper is the third most abundant essential transition metal ion in the human body [7]. Many proteins use copper ions as a cofactor for electron transport, or as a catalyst in oxido-reduction reactions. Copper distribution in the human body is highly controlled, because of its cellular toxicity. An excess of copper ions in living cells can catalyze the production of reactive oxygen species (ROS), which that can damage lipids, nucleic acids, and proteins. Several serious diseases, including Alzheimer's disease [8], Indian childhood cirrhosis (ICC) [9], prion disease [10], and Menkes and Wilson diseases [11], have been associated with the cellular toxicity of copper ions. Due to its extensive applications in our daily lives, copper is also a common metal pollutant. The limit for copper in drinking water, as set by the US Environmental Protection Agency (EPA) is 1.3 ppm, which is a molar concentration of roughly 20 μM.

The development of fluorescent chemosensors for the detection of Cu^{2+} ions has attracted much attention [12–27]. Cu^{2+} is a fluorescence quencher, and so most fluorescent chemosensors detect Cu^{2+} by fluorescence quenching processes, which involve charge or energy transfer mechanisms [15]. However, such processes offer poor sensitivity for metal ion detection; fluorescence enhancement is more easily monitored than fluorescence quenching. This paper reports on a newly designed pyrene-based fluorescence enhancement chemosensor for Cu^{2+} that is based on photoinduced electron transfer (PET). The binding of Cu^{2+} to the chemosensor blocks the PET mechanism and greatly enhances the fluorescence of the pyrene moiety.

In this study, we designed a pyrene-based fluorescent chemosensor, **1**, for metal ion detection. The chemosensor comprises two parts, a pyrene moiety as a reporter, and a benzothiazolenhydrazone component as the metal ion chelator (Scheme 1). Chemosensor **1** exhibits weak fluorescence due to fluorescence quenching by photo-induced electron transfer from nitrogen lone pairs onto pyrene. The binding of a metal ion the chemosensor blocks the PET mechanism, resulting in significant enhancement in pyrene fluorescence. Selectivity testing revealed that Cu^{2+} causes a visible color change in **1**, from light yellow or colorless, and a blue emission on ligation to **1**; no other tested ions produced any significant color change.

2. Materials and methods

2.1. Materials and instrumentations

All solvents and reagents were obtained from commercial sources and used as received without further purification. UV/vis spectra were recorded on an Agilent 8453 UV/vis spectrometer. IR data were obtained on Bomem DA8.3 Fourier-Transform Infrared

* Corresponding author. Tel.: +886 3 5712121x56506.
E-mail addresses: spwu@mail.nctu.edu.tw, spwu@faculty.nctu.edu.tw (S.-P. Wu).

0925-4005/$ – see front matter © 2013 Elsevier B.V. All rights reserved.
http://dx.doi.org/10.1016/j.snb.2013.01.054

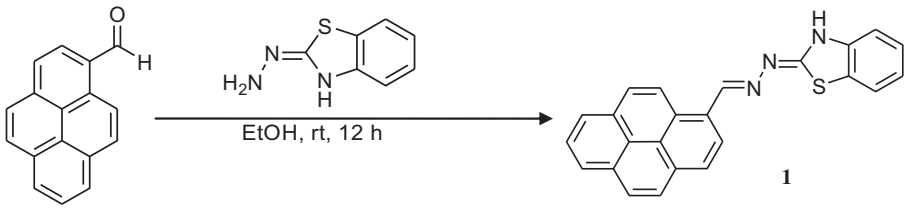

1

Scheme 1. Synthesis of chemosensor **1**.

Spectrometer. NMR spectra were obtained on a Bruker DRX-300 NMR and Varian Unity INOVA-500 NMR spectrometer.

2.2. Synthesis of chemosensor *1*

1-Pyrenecarboxaldehyde (230 mg, 1.0 mmol) and 2-benzothiazolenhydrazone (182 mg, 1.1 mmol) were added to a 10 mL ethanol solution. The reaction mixture was stirred for 12 h at room temperature. The resulting precipitate was collected by filtration and then purified by column chromatography (ethyl acetate:hexane = 1:1) to give **1** as a bright yellow solid. Yield: 336 mg, 89%; m.p. 265.1–267.5 °C; MS (FAB) Found, 378.1 $[M+H]^+$; HRMS (EI) Calcd for $C_{24}H_{15}N_3S_1$, 377.0987; Found, 377.0984. ^1H NMR (300 MHz, DMSO-d_6) δ 12.45 (b, 1H), 9.15 (s, 1H), 8.87 (d, J = 9.3 Hz, 1H), 8.53 (d, J = 8.1 Hz, 1H), 8.38–8.35 (m, 4H), 8.27 (d, J = 9.0 Hz, 1H), 8.22 (d, J = 9.0 Hz, 1H), 8.13 (t, J = 7.5 Hz, 1H), 7.83 (d, J = 7.8 Hz, 1H), 7.49 (d, J = 7.5 Hz, 1H), 7.34 (t, J = 7.2 Hz, 1H), 7.15 (t, J = 7.2 Hz, 1H); ^{13}C NMR (125 MHz, DMSO-d_6) δ 167.1, 131.5, 130.9, 130.7, 130.2, 128.7, 128.2, 128.1, 127.4, 127.3, 127.1, 126.6, 126.5, 126.0, 125.8, 125.7, 125.3, 125.1, 124.3, 123.9, 123.8, 123.7, 122.7, 121.7; FTIR (cm^{-1}) 3183, 3036, 2873, 2809, 1625, 1578, 1445, 1383, 1272, 1135, 840, 743, 710;

2.3. Metal ion binding study by UV–vis and fluorescence spectroscopy

Chemosensor **1** (50 μM) was added with different metal ions (25 μM). All spectra were measured in 1.0 mL acetonitrile–water solution (v/v, 3:1, 5 mM, HEPES buffer, pH 7.0). The light path length of curvet was 1.0 cm.

2.4. The pH dependence on Cu^{2+} binding in chemosensor *1* studied by fluorescence spectroscopy

Chemosensor **1** (50 μM) was added with Cu^{2+} (25 μM) in 1.0 mL acetonitrile–water solution (v/v, 3:1, 5 mM buffer). The buffers were: pH 1–2, KCl/HCl; pH 3–4, CH_3COOH/NaOH; pH 4.5–6, MES/NaOH; pH 6.5–9, HEPES; pH 10–12, Tris/NaOH.

2.5. Determination of the binding stochiometry and the apparent association constants K_a of Cu(II) binding in chemosensor *1*

The binding stochiometry of **1**–Cu^{2+} complexes was determined by Job plot experiments [28]. The fluorescence intensity at 468 nm was plotted against molar fraction of **1** under a constant total concentration. The concentration of the complex approached a maximum intensity when the molar fraction was 0.65. These results indicate that chemosensor **1** forms a 2:1 complex with Cu^{2+}. The apparent association constants (K_a) of **1**–Cu^{2+} complexes was determined by the consequent Eq. (1) [29]:

$$\frac{\alpha^2}{1-\alpha} = \frac{1}{2K_a C_F[M]}, \quad (1)$$

where C_F is the total concentration of chemosensor **1** in the system and α is defined as the ratio between the free chemosensor **1** and the total concentration of chemosensor **1**. The value "α" was obtained using Eq. (2)

$$\alpha = \left[\frac{F - F_0}{F_1 - F_0}\right], \quad (2)$$

where F is the fluorescence intensity at 468 nm at any given Cu^{2+} concentration, F_1 is the fluorescence intensity at 468 nm in the absence of Cu^{2+}, F_0 is the maxima fluorescence intensity at 468 nm in the presence of Cu^{2+}. The association constant K_a was evaluated graphically by plotting $\alpha^2/(1-\alpha)$ against $1/[Cu^{2+}]$. The plot $\alpha^2/(1-\alpha)$ *vs.* $1/[Cu^{2+}]$ is shown in Fig. 6. Data were linearly fitted according to Eq. (1) and the K_a value was obtained from the slope of the line.

2.6. Cell culture

The cell line RAW 264.7 macrophage was provided by the Food Industry Research and Development Institute (Taiwan). RAW 264.7 cells were cultured in Dulbecco's modified Eagle's medium (DMEM) supplemented with 10% fetal bovine serum (FBS) at 37 °C under an atmosphere of 5% CO_2. Cells were plated on 18 mm glass coverslips and allowed to adhere for 24 h.

2.7. Fluorescence imaging

Experiments to assess the Cu^{2+} uptake were performed in phosphate-buffered saline (PBS) with 20 μM $Cu(BF_4)_2$. The cells cultured in DMEM were treated with 10 mM solutions of $Cu(BF_4)_2$ (2 μL; final concentration: 20 μM) dissolved in sterilized PBS (pH = 7.4) and incubated at 37 °C for 30 min. The treated cells were washed with PBS (2 mL) three times to remove remaining metal ions. DMEM (2 mL) was added to the cell culture, which was then treated with a 10 mM solution of chemosensor **1** (2 μL; final concentration: 20 μM) dissolved in DMSO. The samples were incubated at 37 °C for 30 min. The culture medium was removed, and the treated cells were washed with PBS (2 mL) three times before observation. Fluorescence imaging was performed with a ZEISS Axio Scope A1 fluorescence microscope. Cells loaded with chemosensor **1** were excited at 350 nm by using a 50 W Hg lamp. An emission filter of 420 nm was used.

2.8. Quantum chemical calculation

Quantum chemical calculations based on density functional theory (DFT) were carried out using a Gaussian 09 program. Ground state geometry optimization of **1** was performed using the B3LYP functional and the 6-31G basis set. Ground state geometry optimization of **1**–Cu^{2+} complexes was performed using the B3LYP functional and the LANL2DZ basis set.

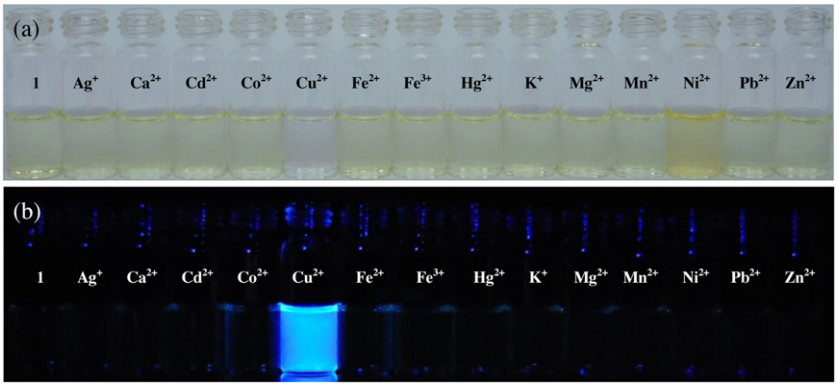

Fig. 1. Color (a) and fluorescence (b) changes of chemosensor **1** (500 μM) after addition of various metal ions (500 μM) in acetonitrile–water (v/v = 3/1, 5 mM HEPES, pH 7.0) solutions. (For interpretation of the references to color in this figure legend, the reader is referred to the web version of the article.)

3. Results and discussion

3.1. Characterization of chemosensor *1*

Chemosensor **1** was synthesized by reaction of 2-benzothiazolenhydrazone and 1-pyrenecarboxaldehyde to form an imine bond between benzothiazolenhydrazone and pyrene (Scheme 1). Chemosensor **1** is yellow and has an absorption band centered at 385 nm, which is red-shifted by 50 nm from the typical pyrene absorption band at 335 nm [30,31]. This is due to longer conjugated double bonds in chemosensor **1**. Chemosensor **1** exhibits weak fluorescence ($\Phi = 0.013$) compared to pyrene ($\Phi = 0.6$–0.9). This results from fluorescence quenching by photoinduced electron transfer from electron lone pairs on nitrogen onto pyrene.

3.2. Cation-sensing properties

We tested the selectivity of Chemosensor **1** by mixing it with Ag^+, Ca^{2+}, Cd^{2+}, Co^{2+}, Cu^{2+}, Fe^{2+}, Fe^{3+}, Hg^{2+}, K^+, Mg^{2+}, Mn^{2+}, Ni^{2+}, Pb^{2+}, and Zn^{2+} metal ions. Cu^{2+} caused a visible color change in **1,** from light yellow or colorless, and had a blue emission (Fig. 1). During Cu^{2+} titration with **1**, the absorbance at 385 nm decreases in intensity, and a new band centered at 330 nm appears. The color change from light yellow to colorless (Fig. 2) clearly indicates the 55-nm blue shift. The new band at 330 nm is close to the absorption band of pyrene, 335 nm. This observation suggests that Cu^{2+} binding with chemosensor **1** blocks conjugation between the double bonds, resulting in a shorter absorption wavelength.

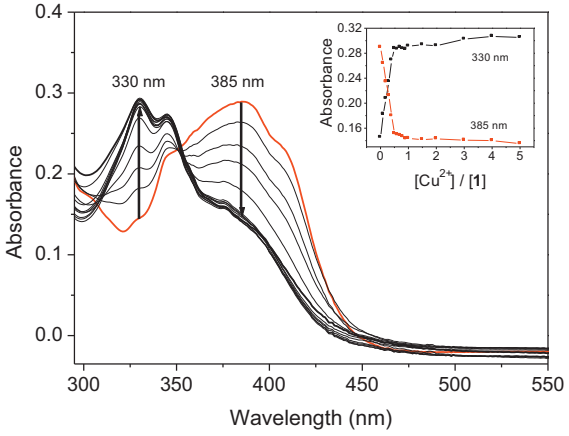

Fig. 2. Changes in the absorption of chemosensor **1** (50 μM) in the presence of various equivalents of Cu^{2+} in acetonitrile–water (v/v = 3/1, 5 mM HEPES, pH 7.0) solutions.

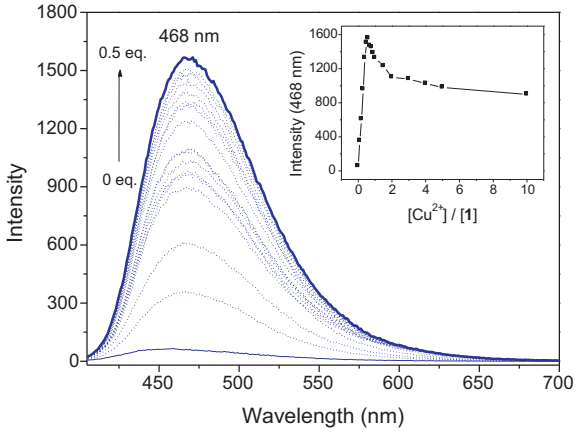

Fig. 3. Fluorescence response of chemosensor **1** (50 μM) to various molar equivalents of Cu^{2+} in acetonitrile–water (v/v = 3/1, 5 mM HEPES, pH 7.0) solutions. The excitation wavelength was 385 nm.

To further evaluate the selectivity of chemosensor **1**, we investigated the fluorescence spectra of chemosensor **1** in the presence of various transition metal ions. Only treatment with Cu^{2+} resulted in a significant blue emission (Fig. 1). During Cu^{2+} titration with chemosensor **1**, a new emission band centered at 468 nm formed (Fig. 3). After adding 0.5 molar equivalents of Cu^{2+}, the emission

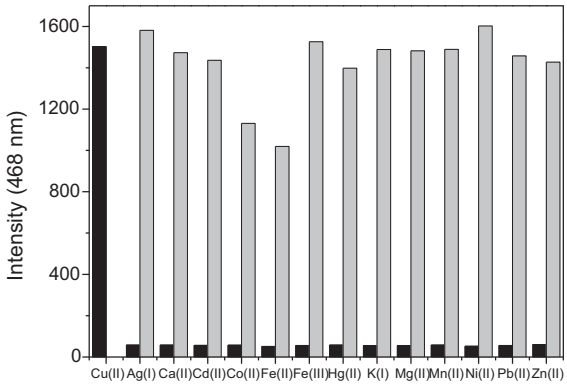

Fig. 4. Fluorescence response of chemosensor **1** (25 μM) to Cu^{2+} (15 μM) or of other metal ions (15 μM) (black bar), and to a mixture of other metal ions (15 μM) with 15 μM of Cu^{2+} (gray bars) in acetonitrile–water (v/v = 3/1, 5 mM HEPES, pH 7.0) solutions.

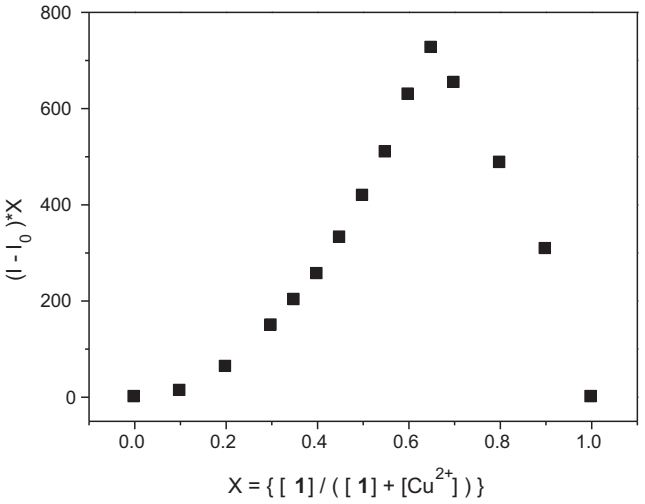

Fig. 5. Job plot of the Cu^{2+}–**1** complexes in acetonitrile–water (v/v = 3/1, 5 mM HEPES, pH 7.0) solutions. The total concentration of **1** and Cu^{2+} was 50.0 μM. The monitored wavelength was 468 nm.

intensity reached a maximum. The quantum yield of the new emission band was 0.49, which is 38-fold that of chemosensor **1** at 0.013. Cu^{2+} was the only metal ion of those we tested that readily binds with chemosensor **1** to yield a significant fluorescence enhancement, suggesting application for the highly selective detection of Cu^{2+} ion.

To study the influence of other metal ions on Cu^{2+} binding with chemosensor **1**, we performed competitive experiments with other metal ions (15.0 μM) in the presence of Cu^{2+} (15.0 μM) (Fig. 4). The observed fluorescence enhancement for mixtures of Cu^{2+} with most metal ions was similar to that seen for Cu^{2+} alone. Reduced fluorescence enhancement was only observed for mixtures of Cu^{2+} and Co^{2+} or Fe^{2+}, indicating that Co^{2+} and Fe^{2+} compete with Cu^{2+} for binding with chemosensor **1**. No other metal ions appeared to interfere with the fluorescence of the chemosensor **1** and Cu^{2+}.

To understand the binding stoichiometry of **1**–Cu^{2+} complexes, we conducted Job plot experiments. In Fig. 5, the emission intensity at 468 nm is plotted against the molar fraction of chemosensor **1** at a constant total concentration of 50.0 μM. Maximum emission intensity was reached for a molar fraction of 0.65, indicating that complexes comprise **1** and Cu^{2+} in a 2:1 ratio; one Cu^{2+} ion binds with two chemosensor **1** molecules. The formation of a Cu^{2+}–$\mathbf{1}_2$ complex was confirmed by ESI-MS, in which the peak at m/z = 815.1 indicates a 2:1 stoichiometry for the $[Cu_2+\mathbf{1}_2–H]^+$ complex (Fig. S3 in the supplementary data). The association constant, K_a, was evaluated graphically by plotting $\alpha^2/(1-\alpha)$ *vs.*

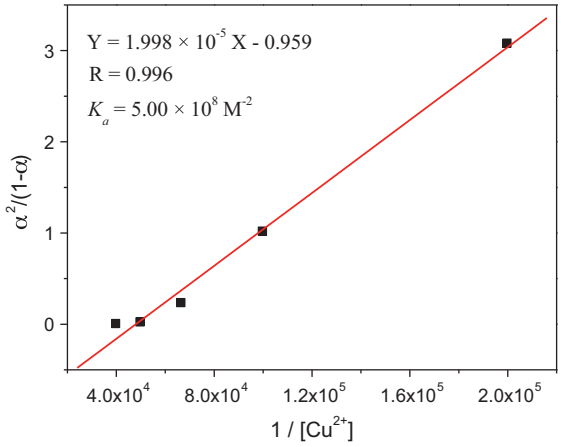

Fig. 6. A binding curve was generated from analysis of fluorescence enhancement measurements, and fitted in accordance with Eq. (1). The association constant, K_a, for Cu^{2+} in chemosensor **1** was 5.0×10^8 M^{-2}.

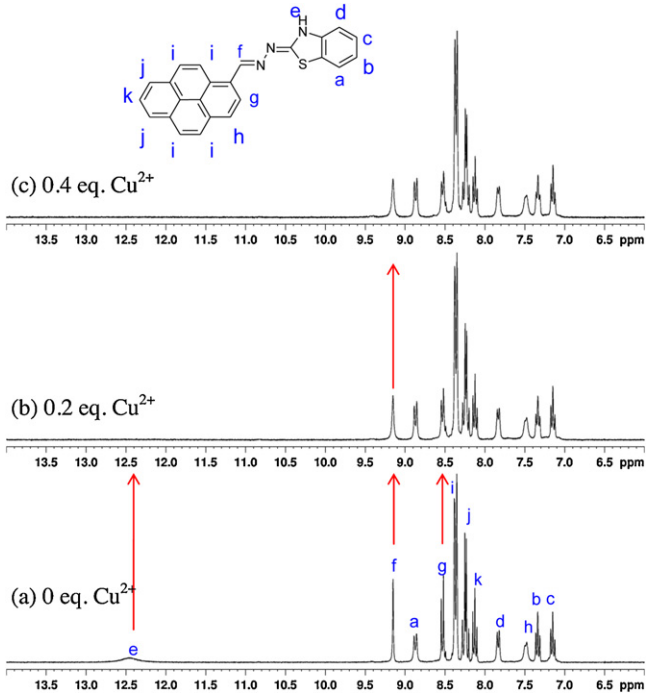

Fig. 7. ^{1}H NMR (300 MHz) spectra of **1** in the presence of Cu^{2+} in DMSO-d_6.

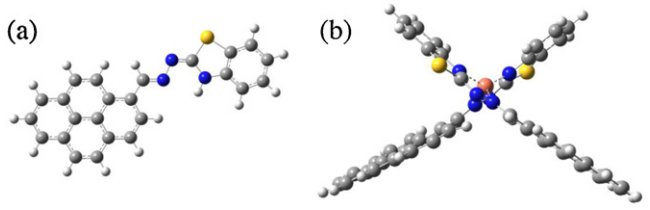

Fig. 8. DFT-optimized structures of (a) **1** and (b) Cu^{2+}–$\mathbf{1}_2$ complexes calculated using the B3LYP/LanL2DZ method (yellow atom, S; blue atom, N; pink atom, Cu). (For interpretation of the references to color in this figure legend, the reader is referred to the web version of the article.)

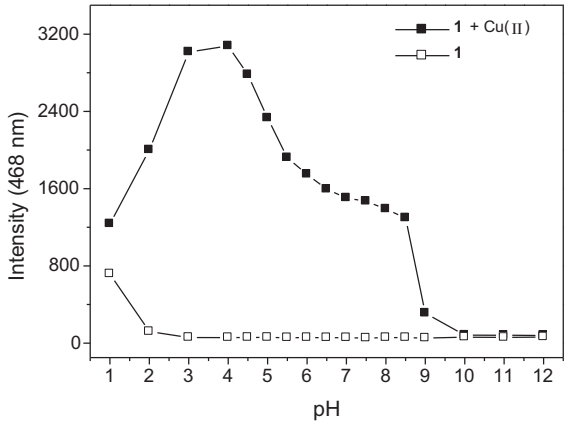

Fig. 9. Fluorescence response (468 nm) of free chemosensor **1** (50.0 μM) (□) and after addition of Cu^{2+} (25.0 μM) (■) in CH_3CN/H_2O (v/v = 3/1, 5 mM buffer) solutions as a function of various pH values. The excitation wavelength was 385 nm.

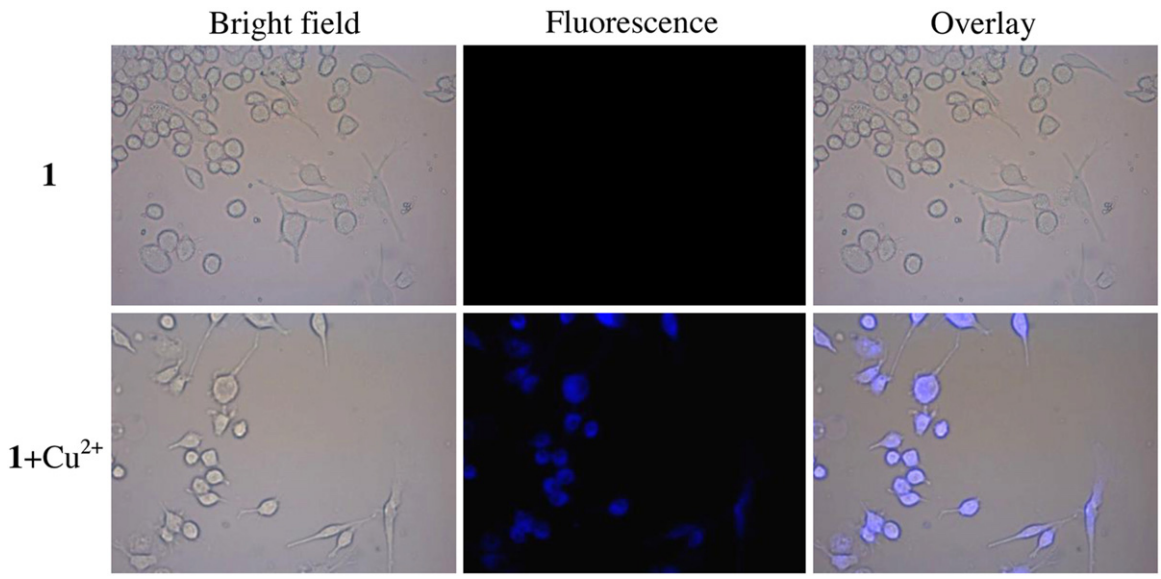

Fig. 10. Fluorescence images of RAW 264.7 cells treated with **1** and Cu^{2+}. (Left) Bright field image; (center) fluorescence image; and (right) overlaid image.

$1/[Cu^{2+}]$, where α is defined as $[F-F_0]/[F_1-F_0]$ (Fig. 6). The data was linearly fitted, and the K_a value was determined from the slope and intercept of the line. K_a for Cu^{2+} binding in chemosensor **1** was found to be $5.0 \times 10^8\ M^{-2}$. The limit of detection for chemosensor **1** as a fluorescent sensor for Cu^{2+} detection was determined from a plot of fluorescence intensity as a function of Cu^{2+} concentration (Fig. S4 in the supplementary data). It was found that chemosensor **1** has a limit of detection of 2.73 μM, which is reasonable for the detection of micromolar concentrations of Cu^{2+} ion, To gain a clearer understanding of the structure of Cu^{2+}–$\mathbf{1}_2$ complexes, we used ^1H NMR spectroscopy. Cu^{2+} is a paramagnetic ion which affects the NMR resonance frequency of protons that are close to the Cu^{2+} binding site. The ^1H NMR spectra of chemosensor **1** revealed that an amine proton (NH) signal at 12.4 ppm almost completely disappears upon the addition of Cu^{2+} (Fig. 7). The proton (H_f) signal at 9.15 ppm became broader after binding with Cu^{2+}, indicating that Cu^{2+} binds to nitrogen at an imine bond. Other peaks remained unchanged. These observations indicate that Cu^{2+} binds to chemosensor **1** through two nitrogen atoms, one of which is an imine.

To elucidate the structure of the Cu^{2+}–$\mathbf{1}_2$ complex, we employed density functional theory (DFT) calculations using the Gaussian 09 software package. Because of the 2:1 ligand-to-metal complexes, as determined from the mass spectrum and Job plot measurements, we applied the B3LYP/LANL2DZ energy optimization routine to determine the possible structure of the Cu^{2+}–$\mathbf{1}_2$ complex. The lowest energy conformations for **1** and Cu^{2+}–$\mathbf{1}_2$ complexes are shown in Fig. 8. Cu^{2+} ligates two chemosensor **1** molecules, and is coordinated by four nitrogen atoms at distances of 2.00, 2.01, 2.12, and 2.18 Å (Fig. S5 in the supplementary data).

We performed pH titration of chemosensor **1** to investigate a suitable pH range for Cu^{2+} sensing. As shown in Fig. 9, the emission intensities of the metal-free chemosensor **1** are very low. After mixing chemosensor **1** with Cu^{2+} in the range of pH 2–8.5, the emission intensity at 468 nm rapidly increases to a maximum. For pH values greater than 9.0, the emission intensity is significantly less than that for the middle pH values, indicating poor stability of the Cu^{2+}–$\mathbf{1}_2$ complexes at high pH. For pH < 2, the enhanced emission does not occur, because of protonation of the amine groups, preventing formation of Cu^{2+}–$\mathbf{1}_2$ complexes.

3.3. Living cell imaging

Chemosensor **1** was used for living cell imaging. To detect Cu^{2+} in living cells, RAW 264.7 cells were cultured in DMEM supplemented with 10% FBS at 37 °C under 5% CO_2. Cells were plated on 18 mm glass coverslips and allowed to adhere for 24 h. RAW 264.7 cells were treated with 20 μM $Cu(BF_4)_2$ for 30 min and washed with PBS three times. The cells were then incubated with chemosensor **1** (20 μM) for 30 min and washed with PBS to remove any remaining sensor. The images of RAW 264.7 cells were obtained using a fluorescence microscope. Fig. 10 shows images of RAW 264.7 cells with chemosensor **1** after treatment with Cu^{2+}. An overlay of fluorescence and bright-field images shows that the fluorescence signals are localized in the intracellular area, indicating subcellular distribution of Cu^{2+} and good cell-membrane permeability of chemosensor **1**.

4. Conclusion

In conclusion, we report a pyrene-based fluorescent chemosensor for Cu^{2+} sensing. We observed significant fluorescence enhancement with chemosensor **1** in the presence of Cu^{2+}. However, adding Ag^+, Ca^{2+}, Cd^{2+}, Co^{2+}, Fe^{2+}, Fe^{3+}, Hg^{2+}, K^+, Mg^{2+}, Mn^{2+}, Ni^{2+}, Pb^{2+}, or Zn^{2+} to the chemosensor solution caused only minimal changes in fluorescence emission. The optimal pH range for Cu^{2+} detection by chemosensor **1** is pH 2–8.5. Chemosensor **1** may have application in fluorescence imaging of living cells. This pyrene-based Cu^{2+} chemosensor provides an effective probe for Cu^{2+} sensing.

Acknowledgements

We gratefully acknowledge the financial support of the National Science Council (ROC) and National Chiao Tung University.

Appendix A. Supplementary data

^1H and ^{13}C NMR spectrum of chemosensor **1**, ESI mass spectra of Cu^{2+}–$\mathbf{1}_2$ and DFT-optimized structure of the Cu^{2+}–$\mathbf{1}_2$ complexes calculated with B3LYP/LanL2DZ method are included in supplementary data. Supplementary data

associated with this article can be found, in the online version, at http://dx.doi.org/10.1016/j.snb.2013.01.054.

References

[1] A.P. de Silva, H.Q.N. Gunaratne, T. Gunnlaugsson, A.J.M. Huxley, C.P. McCoy, J.T. Rademacher, T.E. Rice, Signaling recognition events with fluorescent sensors and switches, Chemical Reviews 97 (1997) 1515–1566.

[2] E.M. Nolan, S.J. Lippard, Tools and tactics for the optical detection of mercuric ion, Chemical Reviews 108 (2008) 3443–3480.

[3] N. Kaur, S. Kumar, Colormetric metal ion sensors, Tetrahedron 67 (2011) 9233–9264.

[4] M. Dutta, D. Das, Recent developments in fluorescent sensors for trace-level determination of toxic-metal ions, Trends in Analytical Chemistry 32 (2012) 113–132.

[5] H.N. Kim, W.X. Ren, J.S. Kim, J. Yoon, Fluorescent and colorimetric sensors for detection of lead cadmium, and mercury ions, Chemical Society Reviews 41 (2012) 3210–3244.

[6] K.J. Wallace, Molecular dyes used for the detection of biological and environmental heavy metals: highlights from 2004 to 2008, Supramolecular Chemistry 21 (2009) 89–102.

[7] J.A. Cowan, Inorganic Biochemistry: An Introduction, Wiley-VCH, New York, NY, 1997, pp. 133–134.

[8] K.J. Barnham, C.L. Masters, A.I. Bush, Neurodegenerative diseases and oxidative stress, Nature Reviews Drug Discovery 3 (2004) 205–214.

[9] S.H. Hahn, M.S. Tanner, D.M. Danke, W.A. Gahl, Normal metallothionein synthesis in fibroblasts obtained from children with Indian childhood cirrhosis or copper-associated childhood cirrhosis, Biochemical and Molecular Medicine 54 (1995) 142–145.

[10] D.R. Brown, Copper and prion disease, Brain Research Bulletin 55 (2001) 165–173.

[11] D.J. Waggoner, T.B. Bartnikas, J.D. Gitlin, The role of copper in neurodegenerative disease, Neurobiology of Disease 6 (1999) 221–230.

[12] Y. Xiang, A. Tong, P. Jin, Y. Ju, New fluorescent rhodamine hydrazone chemosensor for Cu(II) with high selectivity and sensitivity, Organic Letters 8 (2006) 2863–2866.

[13] X. Zhang, Y. Shiraishi, T. Hirai, Cu(II)-selective green fluorescence of a rhodamine–diacetic acid conjugate, Organic Letters 9 (2007) 5039–5042.

[14] G. Li, Z. Xu, C. Chen, Z. Huang, A highly efficient and selective turn-on fluorescent sensor for Cu^{2+} ion based on calix[4] arene bearing four iminoquinoline subunits on the upper rim, Chemical Communication 177 (2008) 4–177, 6.

[15] H.S. Jung, P.S. Kwon, J.W. Lee, J. Kim, C.S. Hong, J.W. Kim, S. Yan, J.Y. Lee, J.W. Lee, T. Joo, S. Kim, Coumarin-derived Cu^{2+}-selective fluorescence sensor: synthesis, mechanisms, and applications in living cells, Journal of the American Chemical Society 131 (2009) 2008–2012.

[16] H.S. Jung, M. Park, D.Y. Han, E. Kim, C. Lee, S. Ham, J.S. Kim, Cu^{2+} ion-induced self-assembly of pyrenylquinoline with a pyrenyl excimer formation, Organic Letters 11 (2009) 3378–3381.

[17] S. Wu, S. Liu, A new water-soluble fluorescent Cu(II) chemosensor based on tetrapeptide histidyl-glycyl-glycyl-glycine (HGGG), Sensors and Actuators B 141 (2009) 187–191.

[18] G. He, X. Zhao, X. Zhang, H. Fan, S. Wu, H. Li, C. He, C. Duan, A turn-on PET fluorescence sensor for imaging Cu^{2+} in living cells, New Journal of Chemistry 34 (2010) 1055–1058.

[19] S. Goswami, D. Sen, N.K. Das, A new highly selective, ratiometric and colorimetric fluorescence sensor for Cu^{2+} with a remarkable red shift in absorption and emission spectra based on internal charge transfer, Organic Letters 12 (2010) 856–859.

[20] S. Wu, T. Wang, S. Liu, A highly selective turn-on fluorescent chemosensor for copper(II) ion, Tetrahedron 66 (2010) 9655–9658.

[21] D. Maity, T. Govindaraju, Highly selective visible and near-IR sensing of Cu^{2+} based on thiourea–salicylaldehyde coordination in aqueous media, Chemistry – A European Journal 17 (2011) 1410–1414.

[22] Z. Xu, L. Zhang, R. Guo, T. Xiang, C. Wu, Z. Zheng, F. Yang, A highly sensitive and selective colorimetric and off–on fluorescent chemosensor for Cu^{2+} based on rhodamine B derivative, Sensors and Actuators B 156 (2011) 546–552.

[23] M.P. Algi, Z. Oztas, F. Algi, Triple channel responsive Cu^{2+} probe, Chemical Communications 48 (2012) 10219–10221.

[24] J. Jo, H.Y. Lee, W. Liu, A. Olasz, C. Chen, D. Lee, Reactivity-based detection of copper(II) ion in water: oxidative cyclization of azoaromatics as fluorescence turn-on signaling mechanism, Journal of the American Chemical Society 134 (2012) 16000–16007.

[25] N.R. Chereddy, S. Thennarasu, A.B. Mandal, A new triazole appended rhodamine chemosensor for selective detection of Cu^{2+} ions and live-cell imaging, Sensors and Actuators B 171–172 (2012) 294–301.

[26] D. Zhang, M. Wang, M. Chai, X. Chen, Y. Ye, Y. Zhao, Three highly sensitive and selective colorimetric and off–on fluorescent chemosensors for Cu^{2+} in aqueous solution, Sensors and Actuators B 168 (2012) 200–206.

[27] B. Hu, Q. Su, P. Lu, Y. Wang, BODIPY modified 9-cycloheptatrienylidene fluorene derivatives: fluorescent turn-on for detecting Cu^{2+} with acidity independence, Sensors and Actuators B 168 (2012) 310–317.

[28] A. Senthilvelan, I. Ho, K. Chang, G. Lee, Y. Liu, W. Chung, Cooperative recognition of a copper cation and anion by a calix[4] arene substituted at the lower rim by a β-amino-α,β-unsaturated ketone, Chemistry – A European Journal 15 (2009) 6152–6160.

[29] V.S. Jisha, A.J. Thomas, D. Ramaiah, Fluorescence ratiometric selective recognition of Cu^{2+} Ions by dansyl-naphthalimide dyads, Journal of Organic Chemistry 74 (2009) 6667–6673.

[30] E. Manandhar, K.J. Wallace, Host–guest chemistry of pyrene-based molecular receptors, Inorganica Chimica Acta 381 (2012) 15–43.

[31] E. Manandhar, J.H. Broome, J. Myrick, W. Lagrone, P.J. Cragg, K.J. Wallace, A pyrene-based fluorescent sensor for Zn^{2+} ions: a molecular 'butterfly', Chemical Communications 47 (2011) 8796–8798.

Biographies

Hsuan-Fu Wang is studying for MS in the Department of Applied Chemistry at National Chiao Tung University.

Dr. Shu-Pao Wu had Ph.D. in 2004, Department of Chemistry, The Ohio State University, USA; Adviser: J.A. Cowan, Postdoctoral Fellow, 2004–2006, College of Chemistry, University of California, Berkeley, USA; Adviser: J.P. Klinman, Assistant Professor, 2006, National Chiao Tung University, Taiwan, Republic of China. Current interests: metal ion chemosensors and AlkB.